remote sensing

Article

Geometrical Variation Analysis of Landslides in Different Geological Settings Using Satellite Images: Case Studies in Japan and Sri Lanka

Suneth Neranjan [1], Taro Uchida [2,*], Yosuke Yamakawa [2], Marino Hiraoka [2] and Ai Kawakami [2]

1 Graduate School of Science and Technology, University of Tsukuba, Tsukuba 305-8572, Japan; suneth.nbro@gmail.com
2 Institute of Life and Environmental Sciences, University of Tsukuba, Tsukuba 305-8572, Japan; yamakawa.yosuke.ga@u.tsukuba.ac.jp (Y.Y.); hiraoka.marino.fu@u.tsukuba.ac.jp (M.H.); kawakami.ai.gn@un.tsukuba.ac.jp (A.K.)
* Correspondence: uchida.taro.fw@u.tsukuba.ac.jp

Abstract: Over the past three decades, Sri Lanka has observed a substantial rise in landslide occurrences linked to intensified rainfall. However, the lack of comprehensive landslide inventories has hampered the development of effective risk analysis and simulation systems, requiring Sri Lanka to rely heavily on foreign-developed models, despite the difficulty of fully examining the similarities between the characteristics of landslides in Sri Lanka and the areas where the model has been developed. Satellite images have become readily available in recent years and have provided information about the Earth's surface conditions over the past few decades. Thus, this study verifies the utility of satellite images as a cost-effective remote-sensing method to clarify the commonalities and differences in the characteristics of landslides in two regions Ikawa, Japan, and Sabaragamuwa, Sri Lanka, which exhibit different geological formations despite similar annual rainfall. Using Google Earth satellite images from 2013 to 2023, we evaluated land-slide density, types, and geometry. The findings reveal that Ikawa exhibits a higher landslide density and experiences multiple-type landslides. In contrast, both areas have similar initiation areas; however, Sabaragamuwa predominantly experiences single landslides that are widespread and mobile. The findings also reveal that various characteristics of landslides are mainly influenced by varied topography. Here, we confirmed that even in areas where comprehensive information on landslides is conventionally lacking, we can understand the characteristics of landslides by comparing landslide geometry between sites using satellite imagery.

Keywords: landslides; landslide geometry; landslide inventory

Citation: Neranjan, S.; Uchida, T.; Yamakawa, Y.; Hiraoka, M.; Kawakami, A. Geometrical Variation Analysis of Landslides in Different Geological Settings Using Satellite Images: Case Studies in Japan and Sri Lanka. *Remote Sens.* **2024**, *16*, 1757. https://doi.org/10.3390/rs16101757

Academic Editor: Sandro Moretti

Received: 19 January 2024
Revised: 3 May 2024
Accepted: 7 May 2024
Published: 15 May 2024

1. Introduction

Landslides are a natural geological phenomenon caused by prolonged weathering and soil formation. Furthermore, landslides have a rapid onset compared with other natural disasters [1]. In particular, most landslides are triggered without any early signs and exhibit rapid movement. Therefore, people do not have sufficient time to take safety measures or evacuate. Thus, a landslide disaster is a risky incident that results in a considerable loss of human life and injury to people, as well potentially severely damaging or destroying infrastructure, agricultural lands, and housing [2]. In the past few decades, socioeconomic issues related to landslide disasters have been increasing because of the rapid development in the mountainous regions and some aspects of climate change such as a change in rainfall pattern and the occurrence of intense rainfall [3].

There are various types of landslides, such as shallow, deep-seated rapid, and deep-seated slow-moving landslides [4]. Furthermore, landslide magnitudes in terms of landslide mass volume differ on the basis of several orders of magnitude. The mobility of landslides is also highly varied [5]. The occurrence of landslides depends on various site conditions, such as the geological conditions of the ground and geomorphology, and triggering events, such as storms and earthquakes. Many researchers have examined the relationship between landslide characteristics and their site characteristics, such as bedrock geology [6] and topography [7]. Therefore, to prevent disasters caused by landslides, it is necessary to use technologies that are suited to landslide characteristics.

Numerous studies have demonstrated a correlation between landslides and topographical characteristics. Previous research indicates a significant association between slope angle and landslide incidence, with varying thresholds observed across different study areas [8–12]. Furthermore, convex slopes exhibit a higher propensity for landslides compared to concave and uniform slopes [13]. Previous studies have also considered factors such as slope aspect, elevation, topographic roughness, and distance from the valley [10,11]. Due to the challenging nature of acquiring data on a large number of landslides, researchers tend to analyze the geometrical characteristics of landslides to comprehend the landslide phenomenon. Key parameters such as area (A), perimeter (P), convex hull-based measure (Ch = A/Ac, where Ac is the area of the convex hull fitted to the polygon), the ratio of area to perimeter (A/P), eccentricity of the fitted ellipse (e), and the ratio of landslide length to fall height are commonly utilized. Through the analysis of variations in these parameters, researchers endeavor to identify triggering mechanisms [14], assess landslide mobility [5,15], and investigate the effects of topography [16,17] on landslides. So, these studies clearly showed the landslide characteristics varied with topography. For landslide mitigation, it is important to understand the type, scale, and mobility of landslides in the target area.

However, there are typically areas with insufficient landslide data or inventories. These regions typically have to depend on foreign-developed landslide risk analysis and simulation systems despite the chances of errors that may occur due to differing geographical landscapes. Moreover, geographical biases exist in the landslide data and inventories. Most landslide studies are limited to young (600–200 million years old) geological formations such as Japan [14], Pacific Northwest of North America [18], China [19], Europe [20], Taiwan [21], and New Zealand [22]. Thus, landslide risk analysis and simulation systems are likely to rely mainly on experience in these areas with sufficient data and inventories. Therefore, it is important to develop methods for clarifying the characteristics of landslides in areas with insufficient data and to accumulate data on the characteristics of landslides in various areas. Remote sensing techniques, such as satellite imagery, enable the retrieval of comprehensive information about landslides across large areas [23,24]. Satellite images have become readily available in recent years and have provided information about the Earth's surface conditions over the past few decades. Several studies have been conducted to develop new technology for detecting and monitoring landslides using satellite images [25–27]. For example, satellite imagery has proven instrumental in landslide studies, as demonstrated using various applications including landslide mapping using FORMOSAT-2 satellite images with an 8 m resolution [28], and SPOT 5 imagery with a 2.5 m resolution [29]. Since 2012, Google Earth has had 0.5 m or over image resolution, including individual houses, industrial facilities, and roads, especially in town areas [30]. Some studies reveal that the RMSE of the Google Earth imagery is 2.18 m and 1.51 m for the horizontal and height coordinates, respectively [31,32] and has an applicability for research [33]. Recently, landslide density has been mapped using open-access satellite radar data in Google Earth Engine [34]. By analyzing the similarities and differences in the landslide characteristics in multiple regions using satellite images with the same precision, it will be possible to provide effective information for applying countermeasure techniques developed in one region to another.

Therefore, the objectives of this study were to (1) verify the utility of satellite images to clarify the commonalities and differences in the characteristics of landslides in two regions, and (2) conduct a case study on interstice comparison between young and old geological regions. This study focuses on two distinct study areas: Ikawa Mountain in Japan and the Sabaragamuwa province in Sri Lanka. Sri Lanka has a very old geology (over 2 billion years old) [35,36] compared with the geologically young previously researched areas. In Sri Lanka, a comprehensive early warning system [37] and hazard zonation mapping are actively undertaken during landslides [38]; however, detailed data and inventories of landslides are still generally lacking [39].

2. Study Area

This study focuses on two distinct study areas: the Ikawa Mountain in Japan (Figure 1a) and the Sabaragamuwa province in Sri Lanka (Figure 1b). As an island tropical country located near the Bay of Bengal and the Indian subcontinent, Sri Lanka receives high rainfall from monsoonal winds (North–West and South–East) and convection rainfall. The country's average annual rainfall varies from 900 mm to 5500 mm. Based on this range of rainfall intensity, the entire area of the country is categorized into three major climate zones (wet, intermediate, and dry). The southeast region of the country shows minimum rainfall, and the southwestern region of the central highland shows the highest rainfall [40]. Because of the high rainfall, Sri Lankan mountains experience extreme rock weathering and soil formation processes, especially in the "wet zone" of the country. Therefore, rainfall-triggered landslides are a common disaster in Sri Lanka. Recent research has indicated that Sri Lanka has an increasing trend of rainfall intensity, and landslides have become a frequent disaster within the last three decades [41,42]. In addition, some studies have shown that changes in land use and cover influence the occurrence of landslides [36].

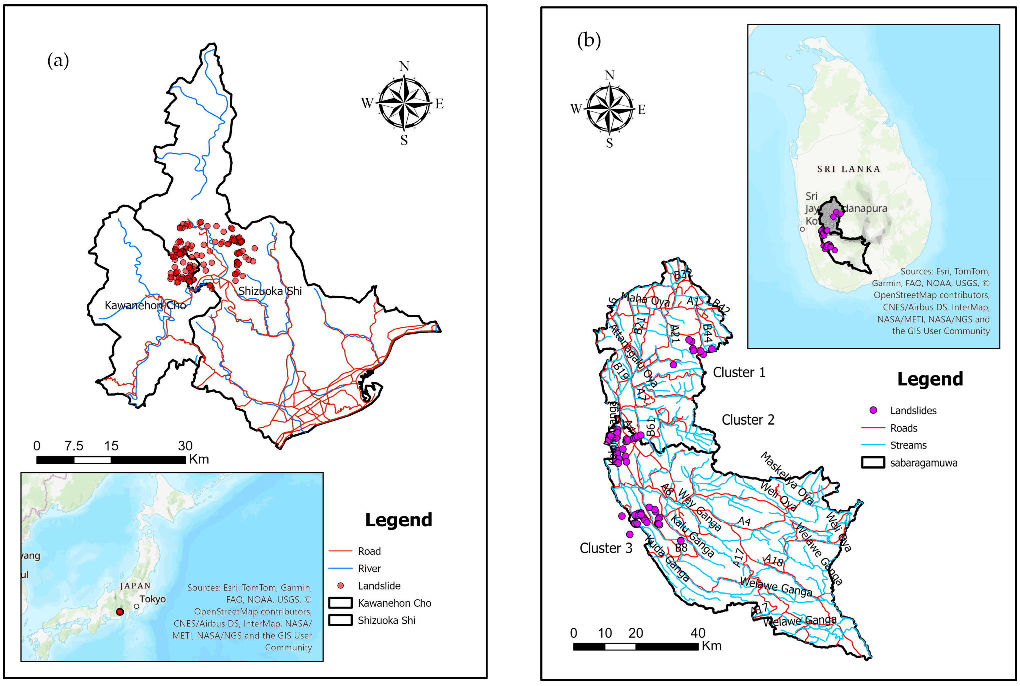

Figure 1. Location of the study areas: (a) Ikawa Mountain, Japan; (b) Sabaragamuwa Province, Sri Lanka (source: Japan Nationwide Municipal Boundary Data https://mapcruzin.com/ (accessed on 31 March 2024); source: Administrative map, Department of Survey, Sri Lanka).

Sabaragamuwa Province, located in the southwest part of the central highlands of Sri Lanka, is characterized by heavy rainfall during the southwest monsoon, resulting in frequent landslides. Recent catastrophic landslide events in the Kegalla district in 2016 and the Rathnapura district in 2017 have left significant imprints on human settlement and the landslides are distinct in Google Earth satellite images. Similarly, the Ikawa area, situated in the southern part of the Minami Alps within Aoi-ku, Shizuoka, Shizuoka Prefecture, Japan, is prone to frequent landslides, evident in satellite imagery. In addition to that, owing to unique geological compositions—sedimentary rocks in Ikawa Mountain and high-grade metamorphic rocks in the Sabaragamuwa province—that contribute to the differences in their landscapes and susceptibility to landslides, these regions have been selected for this study. The research areas chosen for this study comprised 188 km^2 in Ikawa and 715 km^2 in Sabaragamuwa that included three distinct clusters.

2.1. Geology and Geological Age

The Ikawa Mountains in Japan comprise Mesozoic Cretaceous sedimentary rocks, primarily consisting of sandstone, mudstone, and mixed sandstone with mudstone (Figure 2). These sedimentary rocks were formed approximately 60 million years ago on the ocean bed and have been uplifted over an extended period through tectonic events.

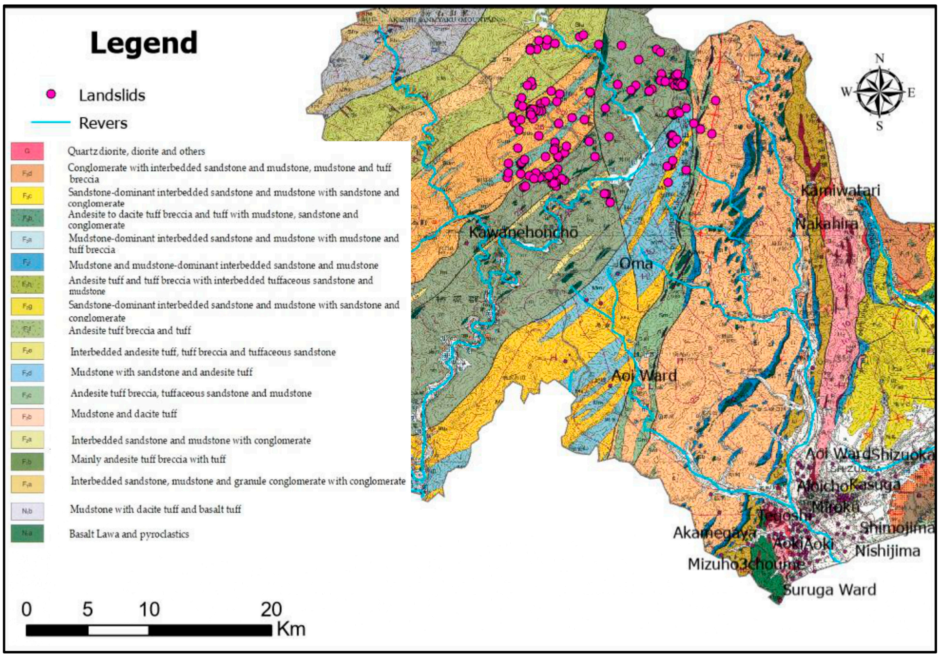

Figure 2. Geology map of the study area in Ikawa, Japan (source: Geological Survey of Japan web page (URL; https://gbank.gsj.jp/data/JPG/GSJ_MAP_G200_NI5432_2010 (accessed on 31 March 2024)).

The Sabaragamuwa province in Sri Lanka is dominated by high-grade Proterozoic metamorphic rocks that date back to more than 1000 million years ago and belong to the Precambrian geological age. These older rocks have undergone intense heat and pressure, resulting in their metamorphosis into high-grade gneissic metamorphic formations (Figure 3) [35].

2.2. Topography and Climate

The Ikawa Mountain area is a high-relief mountain area characterized by steep slopes and deep valleys compared with the Sabaragamuwa province (Figure 4). Hence, in Ikawa, many valleys are incised into the hillslopes, whereas in Sabaragamuwa, the hillslopes are smooth without deep valleys on them.

To evaluate the elevation variation in both study areas, the following analysis was performed. The first step involved selecting the approximate midpoint as the reference point. We then calculated the elevation differences between the highest and lowest points within a given radius from the midpoint using the Digital Elevation Model (DEM). DEMs were generated using 5 m indevel lidar data in Ikawa and a 1:10,000 contour map in Sabragamuwa. Using these data, a triangular irregular network was first generated using ArcGIS 10.8.1, and DEMs were then obtained using ArcScene 10.8.1. The radius of areas with elevation differences was changed from 0.25 km to the end of the study area to explore the spatial variations in elevation across different distances from the central reference point. The topographical analysis revealed that there were small variations in the elevation difference in an area with a radius of 1 km or less, except for Cluster 2 of Sabaragamuwa. However, as the radius of the area increases to 2 or 3 km or more, the increase in elevation difference becomes smaller in Sabaragamuwa. In contrast, an increase in elevation difference was observed until the radius of the area reached 5 km in Ikawa (Figure 5). Thus, Ikawa Mountain exhibits an elevation difference of 1863 m over a distance of 6 km, and Sabaragamuwa exhibits a small elevation difference (Cluster 1: 1145 m; Cluster 2: 516 m; Cluster 3: 908 m) (Figure 5). These results show that although there is no major difference in the slope gradient of the two regions when viewed over a narrow area (ca. <1 km), Ikawa has a longer slope than Sabaragamuwa.

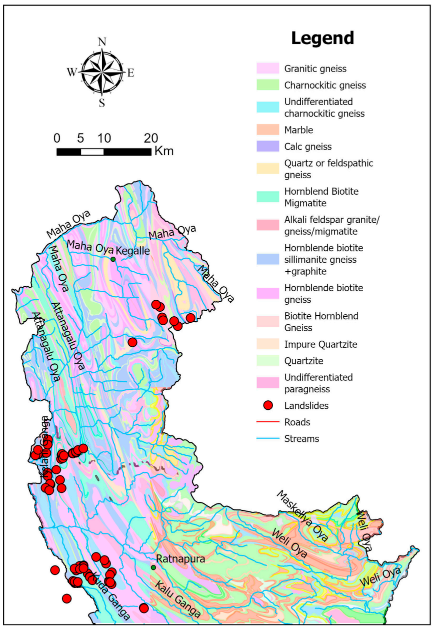

Figure 3. Geology of the study area in Sabaragamuawa, Sri Lanka (Source: 1:100,000 Geology map published by Geological Survey and Mining Bureau, Sri Lanka).

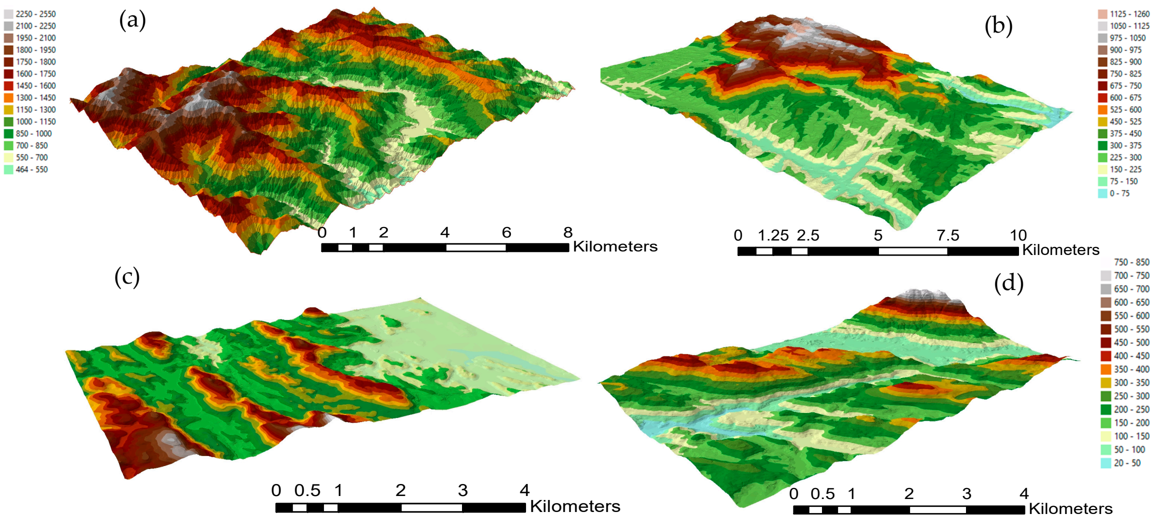

Figure 4. Topography of the study areas: (**a**) Ikawa; (**b**) Cluster 1, Sabaragamuwa; (**c**) Cluster 2, Sabaragamuwa; (**d**) Cluster 3, Sabaragamuwa.

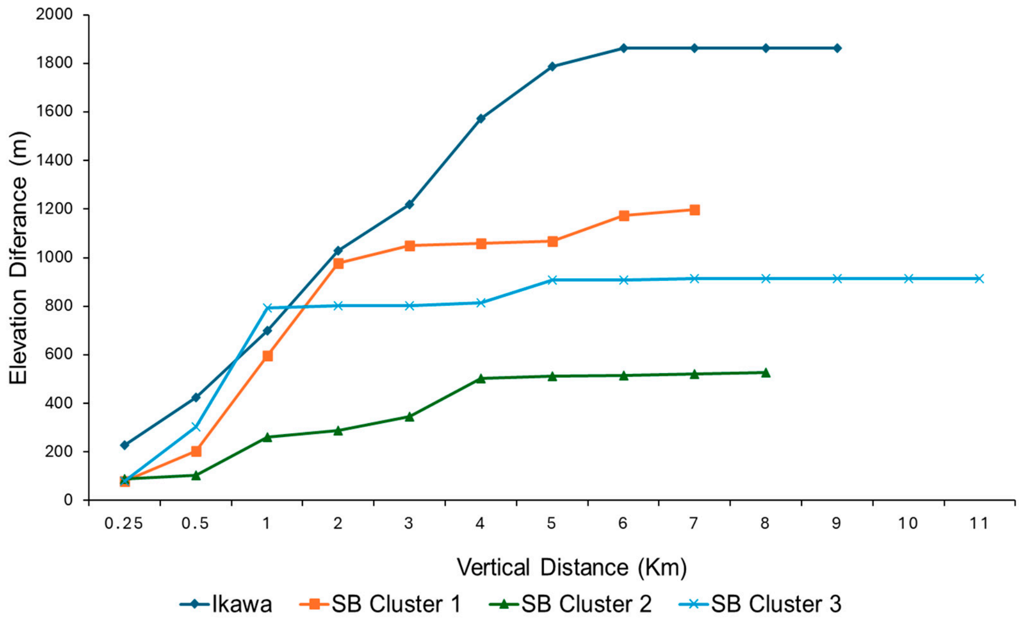

Figure 5. Elevation difference with distance of study areas (SB: Sabaragamuwa).

Furthermore, the climate of both study areas plays a crucial role in triggering landslide events. Ikawa Mountain experiences its heaviest rainfall during the typhoon season, which typically occurs from June to October, with an average annual rainfall of 3117 mm. Remarkably, 73% of the annual rainfall in Ikawa Mountain is concentrated within this period. Conversely, the Sabaragamuwa province receives its heaviest rainfall during the monsoon season, which spans from May to September, with an average annual rainfall ranging from 2500 to 4000 mm. Hence, unlike Ikawa Mountain, rainfall in the Sabaragamuwa province is more evenly distributed throughout the monsoon, rather than being concentrated within a specific period.

In addition, the field survey revealed distinct differences between Ikawa and Sabaragamuwa. Specifically, Ikawa exhibited a thicker soil overburden than Sabaragamuwa. Furthermore, the soil in Ikawa contained coarse sand and rock fragments, whereas the soil in Sabaragamuwa consisted of fine sand with a higher clay content. Consequently, the landslides in Sabaragamuwa contained a greater amount of soil than the landslides in Ikawa, occasionally incorporating large boulders. In contrast, the sedimentary rocks in Ikawa were observed to be highly fractured, resulting in Ikawa landslides containing more rock fragments than Sabaragamuwa landslides.

3. Materials and Methods

This study employed a methodology of mapping landslide geometrical data using Google Earth's satellite images and ArcGIS 10.8.1 software (Figure 6). The individual examination of landslides to plot landslide locations and areas within the study area was conducted using Google Earth Pro satellite images captured from 2013 to 2023. In this study, we determined the size of one pixel in the satellite images used for georeferencing the national grid (JGD_2000 and SLgrid99). As a result, the resolution of images used in this study were 0.1~0.3 m at Ikawa and 0.15~0.7 m at Sabaragamuwa (Table 1).

Landslides were identified on the basis of contrasts in exposed soil or rock surfaces, common geomorphic landslide features, and vegetation characteristics. Mapping includes the headscarp and the lowest point of the entire landslide, considering connected or coalesced landslides with multiple mapping points. In this study, we characterized landslides on the basis of their connectivity (Figure 7). We classified them into three types: single, connected, and coalescing landslides.

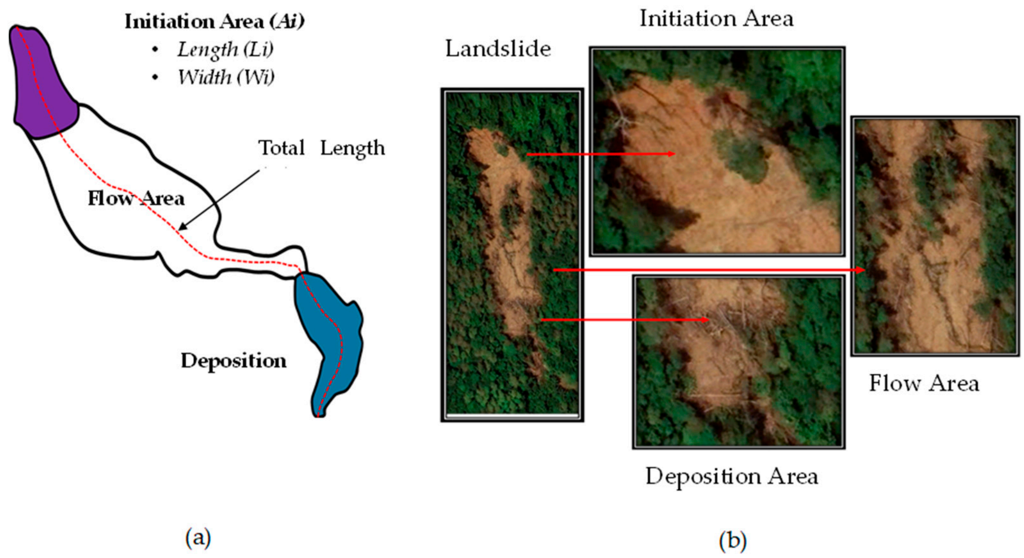

Figure 6. (**a**) Major features of the landslide; (**b**) identifying landslide features in satellite images, source: Google Earth.

Table 1. Frequency and distribution of landslides by region.

Study Area	Landslide Type	Number of Landslide Polygons	Number of Mapped Initiation Area Polygons	Number of Headscarp Points	Remark
Ikawa, Japan,	Single	146	91	146	91 landslides were selected for analysis
	Connected	9	0	21	
	Coalescing	12	0	51	
	Total	167	91	218	
Sabragamuwa, Sri Lanka,	Single	59	59	59	59 landslides were selected for analysis
	Connected	3	0	6	
	Coalescing	0	0	0	
	Total	62	59	65	

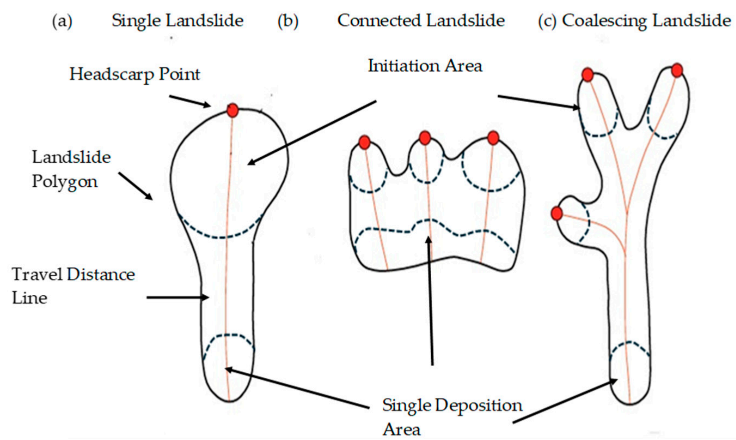

Figure 7. Types of landslides are based on connectivity characteristics.

We conducted a thorough comparison of the landslide geometrical characteristics. Considering the complex geometry of multiple-type landslides, the geometry of single-type landslides was compared to determine similarities and differences in landslides in each study area. For single landslides, the initiation, flow, and deposition areas were identified, demarcating the landslide boundaries on the basis of inherent features (Figure 6). However, the initiation area of some landslides could not be identified because of the low image resolution and obstruction from tree branches. Certain landslides intersecting water discharge in wide valleys or streams were excluded from this study.

Parameters such as the landslide total area (At), initiation area (Ai), total length (Lt), initiation area length (Li), and initiation area width (Wi) were measured for single landslides using geographical information systems. This study considered the landslide length along the flow path and the maximum width of the initiation area as the landslide width. Landslide mobility is generally described using the ratio between the landslide fall height (H) and travel distance (L). On the basis of the H/L value, landslide mobility was estimated [5]. In this study, landslide mobility was investigated using the ratios of total length to initiation area length (Lt/Li) and total area to initiation area (At/Ai) to understand the landslide travel distance and spread compared with the initiation area. Basic statistics in Microsoft Excel were used to identify similarities and differences.

This study employed a grid-wise analysis approach to investigate the spatial distribution of landslides in the study areas, using 1 km square grids as spatial units. Using ArcGIS, the number of landslides, identified using headscarp points within each grid, was counted. The methodology involved identifying and categorizing different landslide types within the study areas, delineating their spatial extent, and calculating the percentage distribution of each type [5].

The Ikawa area consists of various types of mudstones and sandstones (Figure 2); thus, we tested the effect of bedrock geology on landslide geometry in the Ikawa dataset. All types of mudstones were considered mudstones, and all types of sandstones were considered sandstones.

4. Results

4.1. Comparative Analysis of Landslide Characteristics Based on Rock Study Areas

In Ikawa Mountain, 146 single landslide polygons, 9 connected landslide polygons, and 12 coalescing landslide polygons were mapped. The total mapped landslides were 167, and due to the multiple initiation areas of connected and coalescing landslides, the total landslide initiation areas were found to be 218. In Sabaragamuwa, 59 single landslide polygons and 3 connected landslide polygons were mapped, resulting in 62 landslide polygons and 65 initiation areas (Table 1).

In Ikawa, 87.4% were single landslides, characterized by individual occurrences, whereas 7.2% were coalescing landslides, involving the merging of two or more landslides, and 5.4% were connected landslides (Figure 8a). In Sabaragamuwa, 95.1% were single landslides, characterized by individual occurrences, and 4.8% were connected landslides (Figure 8b).

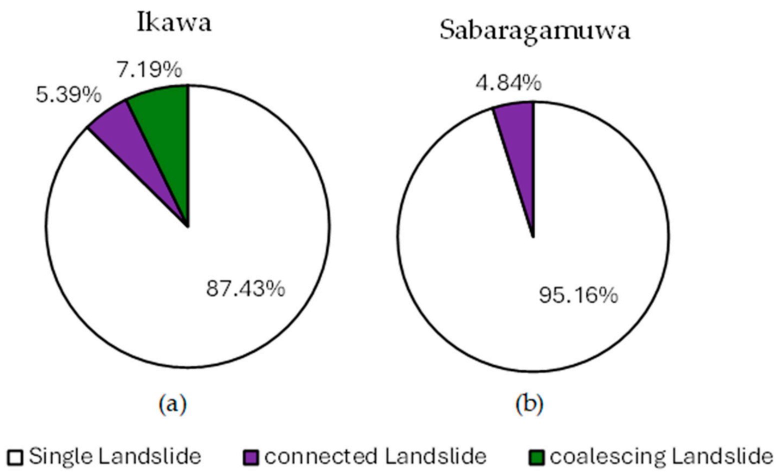

Figure 8. Landslide types of study areas: (**a**) landslide types in Ikawa, Japan; (**b**) landslide types in Sabaragamuwa, Sri Lanka.

4.1.1. Landslide Density

In Ikawa, 66.8% of 1 km cells exhibit no landslides. In addition, 13.9% have one landslide, whereas the remaining cells exhibit multiple landslides (2–15 in number) (Figure 9a). In Sabaragamuwa, 89.6% of cells do not experience landslides, indicating a generally lower occurrence than in Ikawa. However, 7.3% have one landslide, and the remaining grids with landslides show multiple events (from two to four in number) (Figure 9b). In Ikawa, 5.7% of the cells had five or more headscarps, whereas in Sabaragamuwa, no cells had five or more landslides.

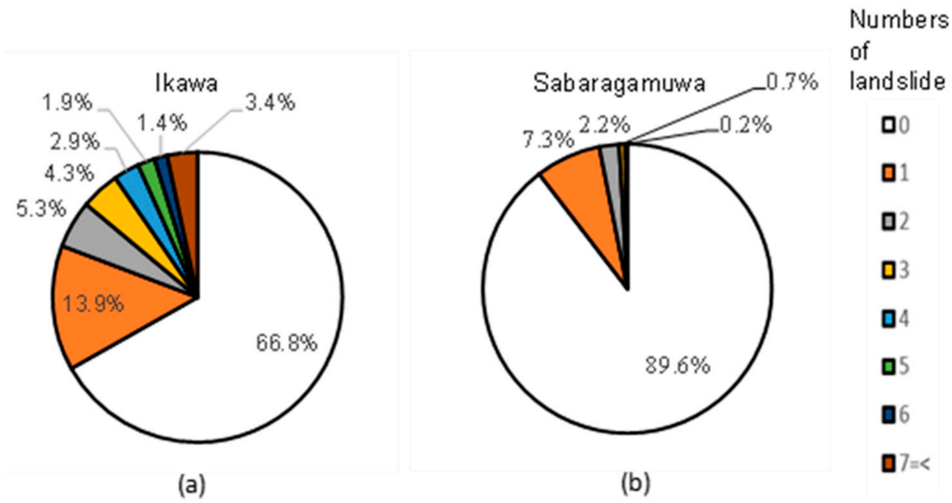

Figure 9. Landslide density of study areas: (**a**) landslide density in Ikawa, Japan; (**b**) landslide density in Sabaragamuwa, Sir Lanka.

4.1.2. Landslide Geometry

Considering the difficulty in determining the initiation area of 55 landslides in Ikawa, 91 single landslides were included in this study (Table 1). In Ikawa, the median of the entire area is 2669 m^2, ranging from 102 to 9571 m^2, whereas Sabaragamuwa exhibits a higher median of 4887 m^2, ranging from 395 to 26,731 m^2. This difference indicates that on average the landslides in Sabaragamuwa cover a larger area, as emphasized by the wider interquartile range (Q3-Q1 = 11,364 m^2), than those in Ikawa (Q3-Q1 = 3819 m^2). The initiation area box plot reveals a higher median in Sabaragamuwa (1282 m^2) than in Ikawa (929 m^2), indicating larger initiation areas for landslides in Sabaragamuwa. However, the difference in initiation area shows a lower difference than the difference in total area of the landslides. The interquartile ranges of the initiation areas in Ikawa and Sabaragamuwa were 11,368 and 2292 m^2, respectively (Figure 10).

Sabaragamuwa exhibits larger dimensions with a median total length of 183 m when compared with Ikawa's 115 m. Quartiles (Q1 = 101 m; Q3 = 291 m) and maximum length (562 m) in Sabaragamuwa consistently exceed those in Ikawa (Q1 = 22 m, Q3 = 180 m, and Max = 329 m). The initiation area length in Sabaragamuwa (median = 49 m) slightly surpasses that in Ikawa (median = 46 m), with quartiles (Q1 = 31 m; Q3 = 80 m) and maximum values (129 m) being slightly higher in Sabaragamuwa than in Ikawa (Figure 11a,b). The landslide initiation area width measurements illustrate that both study areas have nearly similar ranges. Ikawa and Sabaragamuwa have median values of 29 m and 34 m and interquartile ranges of 20–45 m and 21–45 m, respectively (Figure 11c).

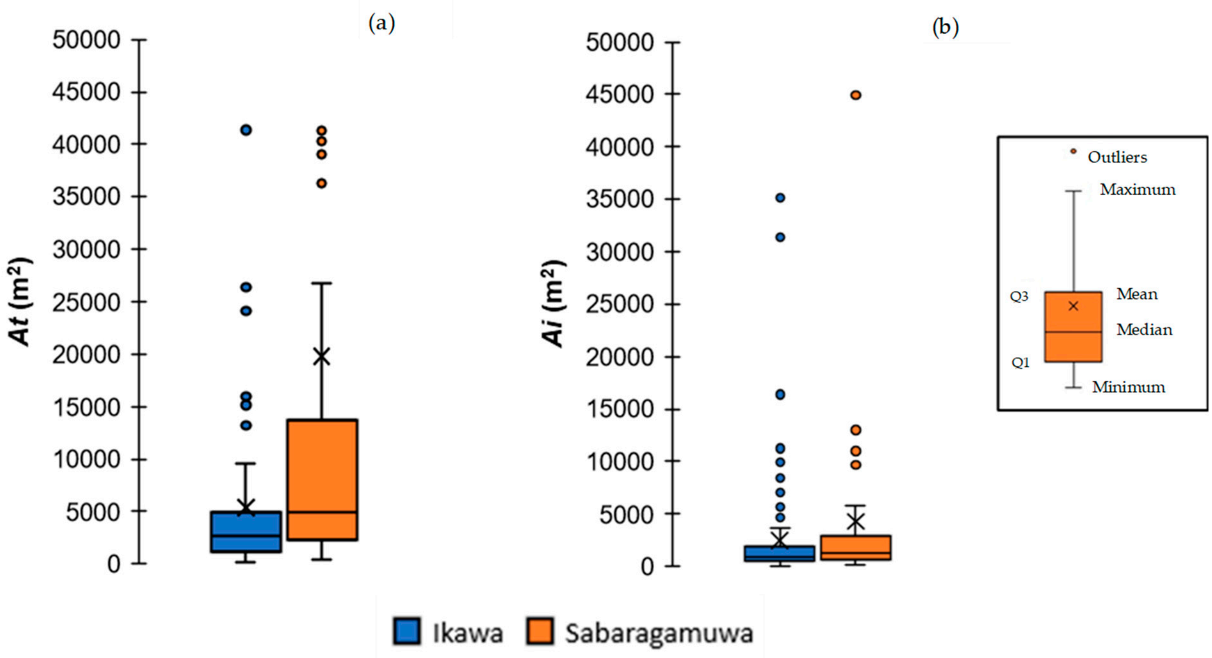

Figure 10. Box plot of landslide shape index: (**a**) whole area; (**b**) initiation area.

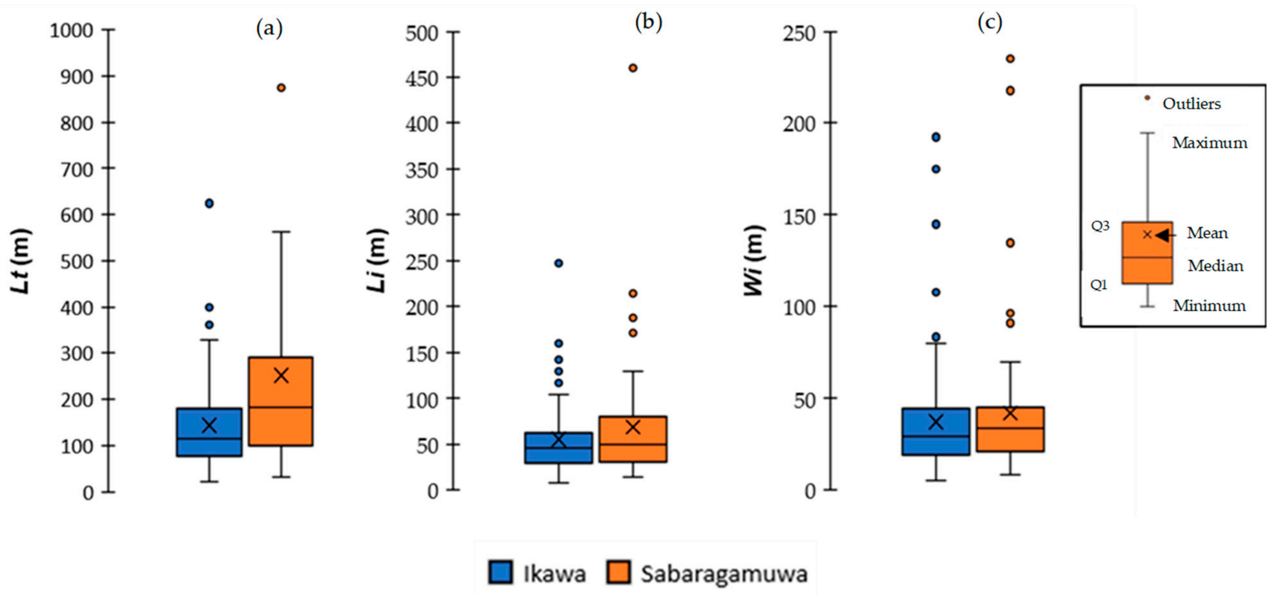

Figure 11. Box plot of landslide shape index: (**a**) *Lt*; (**b**) *Li*; (**c**) *Wi*.

4.1.3. Landslide Mobility

In Ikawa, the At/Ai ratio ranges from 1.26 to 4.68, with a median of 2.60, whereas, in Sabaragamuwa, it ranges from 1.51 to 7.94, with a median of 3.94. The Lt/Li ratio in Ikawa ranges from 1.01 to 4.72, with a median of 2.45, whereas, in Sabaragamuwa, it ranges from 0.76 to 6.77, with a median of 3.27. These findings indicate that landslide mobility is higher in Sabaragamuwa than in Ikawa (Figure 12).

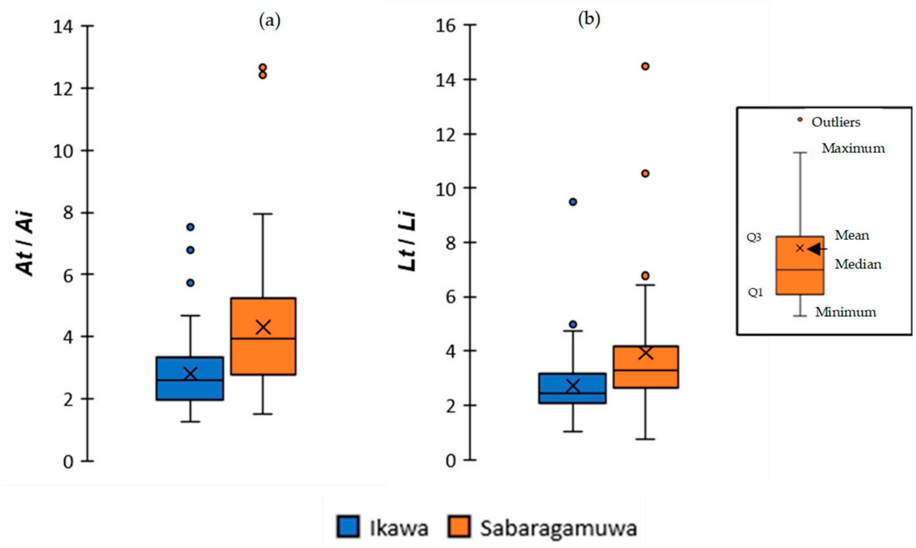

Figure 12. Box plot of landslide mobility: (**a**) *Lt*/*Li*; (**b**) *At*/*Ai*.

4.2. Comparative Analysis of Landslide Characteristics Based on Rock Types in Ikawa

4.2.1. Landslide Type

Mudstone exhibits the highest percentage of connected landslides (9%) and a moderate percentage of coalescing landslides (7%). This indicates that mudstone has a higher tendency to form multiple landslide events. Sandstone has the highest percentage of single landslides (93%) and no connected landslides. This indicates that landslides occurring in sandstone areas are more likely to be isolated events than those occurring in mudstone areas (Figure 13).

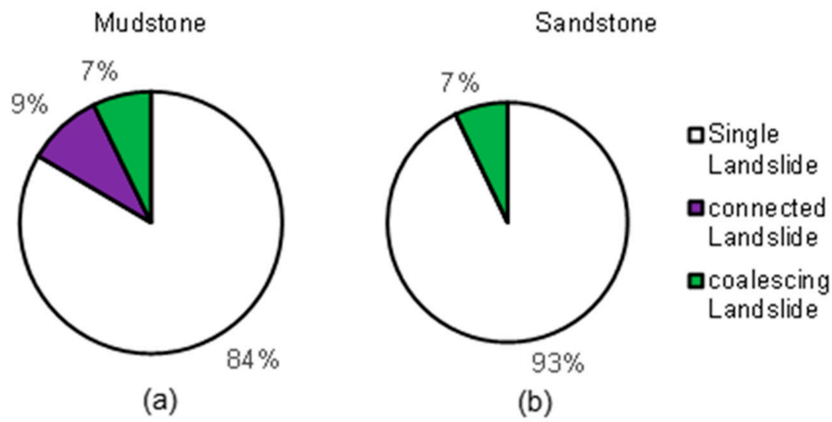

Figure 13. Comparative analysis of landslide types: (**a**) landslide types in mudstone; (**b**) landslide types in sandstone.

4.2.2. Landslide Density

The grid-based density analysis of landslides was performed on different rock types in Ikawa. For mudstone, 68% of the grids exhibit no landslides; conversely, 13% have a single landslide, and 19% exhibit more than one landslide. For sandstone, 55% of the grids are landslide-free, 17% have one landslide, and 28% display a higher tendency for multiple landslides than mudstone. Comparatively, sandstone exhibits a slightly higher landslide occurrence than mudstone (Figure 14).

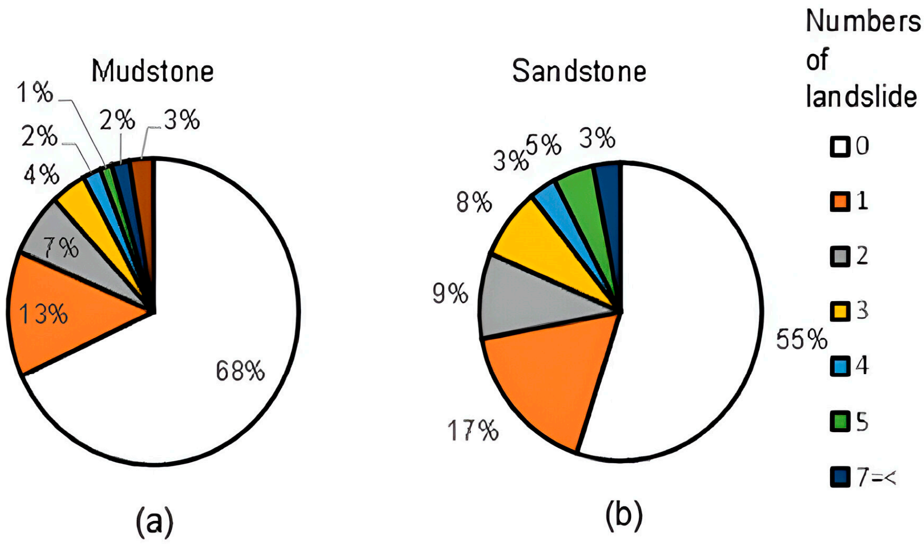

Figure 14. Landslide density based on rock types: (**a**) landslide density in mudstone; (**b**) landslide density in sandstone.

4.2.3. Landslide Geometry

In the entire area, mudstone displays a wide range of area from 102 to 15,991 m^2, with a median of 3807 m^2. Landslides occurring in sandstone have a smaller total area than mudstone, ranging from 473 to 5882 m^2, with a median of 2571 m^2. In the initiation area, landslides occurring in mudstone range from 27 to 7088 m^2, with a median of 1181 m^2. In contrast, the sandstone initiation areas are smaller, varying from 138 to 1940 m^2, with a median of 856 m^2 (Figure 15).

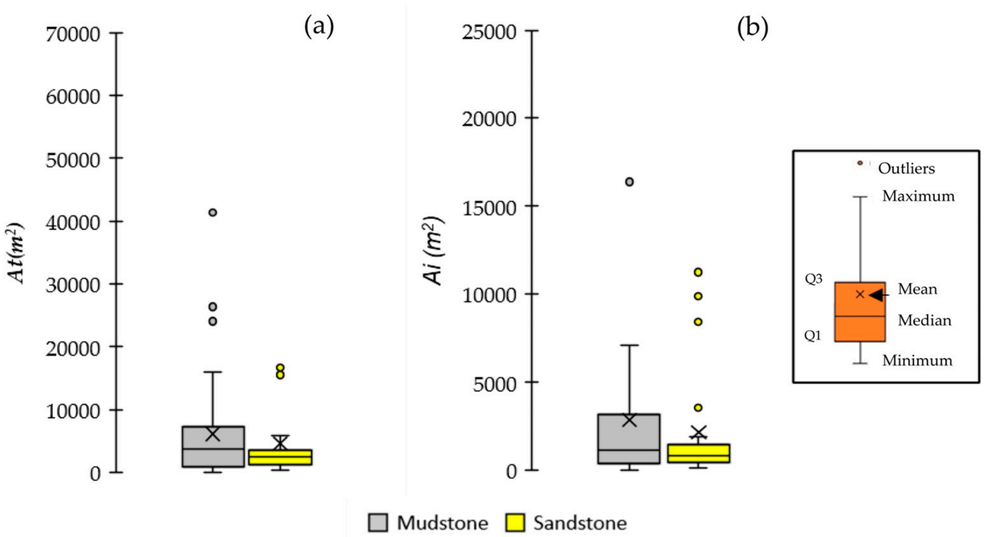

Figure 15. Comparison of landslide shape index parameters in mudstone and sandstone landslides using box plots for (**a**) *At* and (**b**) *Ai*.

For the total length, landslides in mudstone have a broad length range of 22 to 403 m, with a median of 1127 m. Sandstone landslides generally have shorter total lengths than mudstone landslides ranging from 33 to 277 m, with a median of 104 m. The initiation area length of landslides occurring in mudstone displays lengths ranging from 7 to 160 m, with significantly narrower widths (Figure 16).

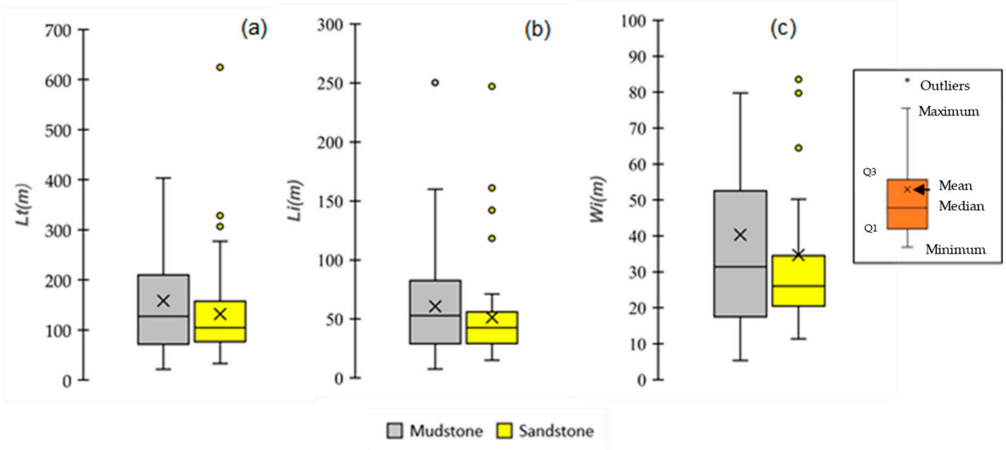

Figure 16. Comparison between mudstone and sandstone landslides based on landslide shape index parameters using box plots for (**a**) *Lt*; (**b**) *Li*; and (**c**) *Wi*.

4.2.4. Landslide Mobility

The analysis of boxplots for the ratios of landslide total length to initiation area length and landslide total area to initiation area provides information about the variation mobility characteristics of landslides based on different rock types. Mudstone landslides exhibit a moderate range of total length to initiation area length ratios (1.01–4.72), indicating moderate mobility. Sandstone landslides generally have lower ratios (1.43–4.27) (Figure 17).

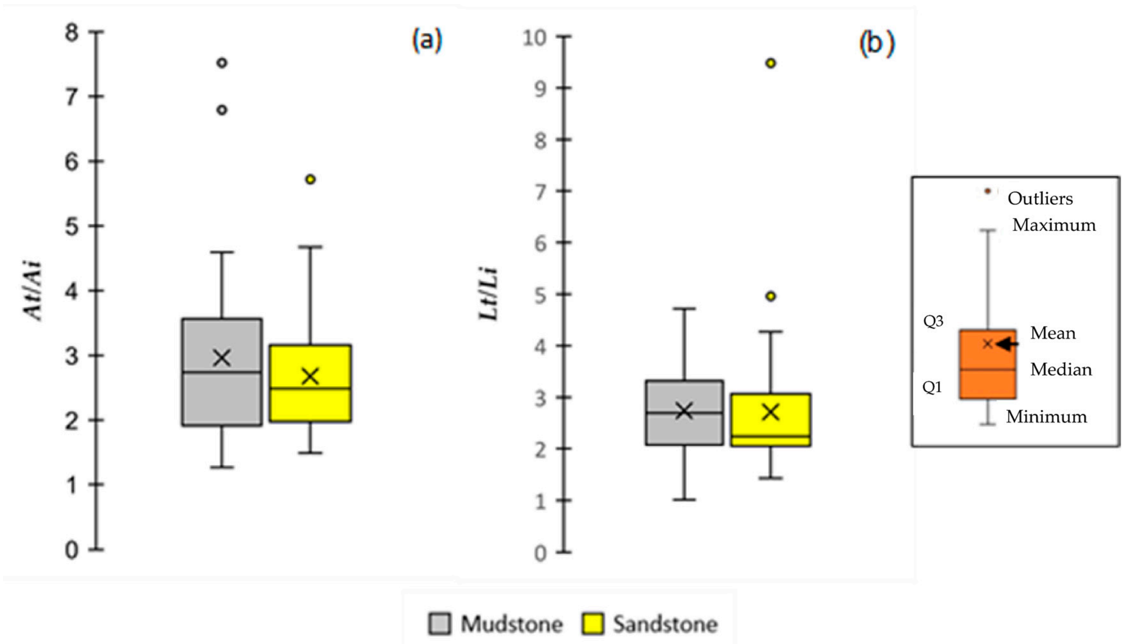

Figure 17. Comparison of landslide mobility parameters in mudstone and sandstone landslides with box plots regarding (**a**) *Lt*/*Li* and (**b**) *At*/*Ai*.

5. Discussion

5.1. Roles of Resolution of Images

The satellite images had varying resolutions, but the differences between images of the same area were minimal (refer to Table 1). Therefore, it is believed that the impact of image resolution on the interpretation of each region is insignificant. The results of this study, i.e., Figures 7–17, were composited interpretation results using multiple images, but we do not think that the effect of using multiple images from different times is a particularly large difference from the perspective of resolution.

However, there was a systematic difference in the resolution of satellite images between Ikawa and Sabaragamuwa (Table 1). The minimum calculated area for landslide initiation in Ikawa was 27 m^2, with 75% of the measured area exceeding 472 m^2. In the Sabaragamuwa study area, the minimum starting area was 165 m^2, with 75% of measurements greater than 649 m^2. Additionally, the minimum width and length values were 5 m and 7 m in Ikawa, and 8 m and 14 m in Sabaragamuwa. Even in Sabaragamuwa, where the resolution is coarse, these landslides are several times larger than a single pixel. Therefore, we believe that our landslides are sufficiently large compared to the pixel size. Although further investigation is required, such as a comparison with results using other highly accurate methods, we currently believe that the difference in image resolution has little effect on the similarities and differences in the landslides that have been clarified. This agrees with recent previous studies. Likewise, Google's satellite imagery has been effectively utilized in various landslide studies, including the creation of landslide inventories in Mexico [43], susceptibility assessments in Afghanistan [44], and detailed mapping in Creta Island, Greece [45]. These previous studies and our results indicate that high-resolution satellite images may be an effective tool for research on landslides in areas where landslide inventories are not sufficiently stored.

5.2. Similarity and Difference in Landslide Activity Revealed Using Satellite Image Interpretation

The inter-site comparison of landslide characteristics between Ikawa, Japan, and Sabaragamuwa, Sri Lanka reveals that although the scale of the initiation areas was similar, there were significant differences in flow and deposition parts and density using satellite images. Moreover, the comparison between the sandstone and mudstone areas in Ikawa revealed that although the indices of landslide mobility (i.e., At/Ai and Lt/Li) were similar in both areas, the scale of the initiation area and density differed.

In contrast, various studies suggest that rock types significantly impact the occurrence and types of landslides. For example, previous research indicates that marine volcaniclastics have high mobility, while submarine basalt and chert are less prone to movement [5]. Shallow landslide density also varies with rock type, with fewer landslides in Paleozoic sedimentary rock areas and many more in granite regions [6]. Moreover, shale-dominated complexes are known to have a higher frequency of shallow landslides, contributing to a greater overall landslide susceptibility. Deep-seated landslides, while pre-dominantly found in shale-dominated areas, are occasionally observed in more resilient sandstone-dominated zones, though with less frequency [46]. The findings of this study, which demonstrated no significant discrepancies in characteristics such as the magnitude of landslides between the two regions with starkly disparate geological ages, appear to challenge the conclusions of previous studies. Although the reason for this discrepancy requires further investigation, one possible explanation is that the landslide geometry is not solely determined by geological conditions. In other words, it is hypothesized that various conditions, including climate and tectonic activities, exert a complex influence. That is, the results of this study may indicate that even if the geological conditions differ significantly, the effects of the differences in geological conditions may be canceled out by other factors.

The reasons for the differences in the geometrical characteristics of each part are as follows: The mean values of the percentage slopes in Ikawa show high values for all three sections of the landslides (initiation area: 86.2% (40.8°); flow area: 89.2% (41.7°); deposition area: 89.2%). However, in Sabaragamuwa, the landslide initiated on a higher slope and ended with a gentle slope (initiation area: 84.7% (40.3°); flow area: 74.2% (36.6°); deposition area: 60.2% (31.1°)) (Figure 18). Moreover, 25% of the landslides were deposited on a gentle slope with less than 25% (14.1°) in Sabaragamuwa, whereas no landslide was deposited on such a gentle slope in Ikawa.

These results indicate that most of the landslides in Ikawa were stopped in valleys that developed on large, steep slopes (Figures 4 and 5), whereas some of the landslides in Sabaragamuwa flowed down to the bottom of slopes where the slopes became gentler. In other words, landslides in Ikawa flowed and were deposited in deep incised valleys and valley walls, restricting the spread of landslides with narrow flow paths and smaller deposition areas.

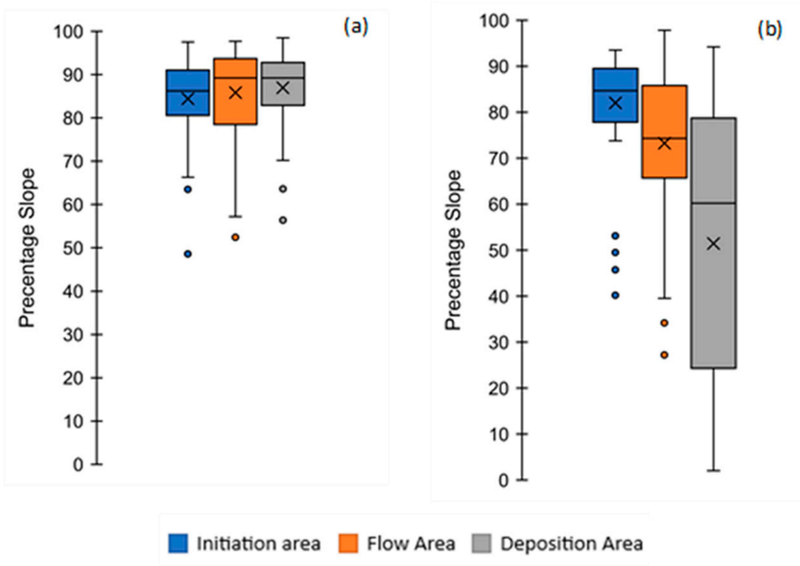

Figure 18. Review of percentage slope in landslide initiation area, flow area, and deposition area: (**a**) Ikawa; (**b**) Sabaragamuwa.

In contrast, in Sabaragamuwa, the landslides were facilitated in spreading by having wider flow paths and deposition areas because the valley was not developed on slopes, and the landslide reached the bottom of the slope. In addition to valley development, this difference may also be controlled by slope size, suggesting that the slope in Ikawa was very long; thus, the landslide traveled long distances to reach the bottom.

Furthermore, the difference in topography controlled the connectivity of the landslide. It is possible to argue that the higher trend in the occurrence of multiple landslides mainly depends on valley density. This trend is because a connected valley provides the possibility of connecting two or more landslides. However, because of the "geologically old" landscape, Sabaragamuwa consists of a more eroded and wider valley than Ikawa. Therefore, there are no more connected valleys, and there is less possibility of connecting landslides. Consistent with the relevant research, the formation of multiple landslides predominantly depends on topography, particularly in the case of coalescing landslides formed by interconnected valleys [5].

5.3. Characteristics of Landslide in the Area with Very Old Geological Formation

Most previous landslide studies have been conducted in areas underlain by young (i.e., 600–200 million) geological formations, such as Japan, the Pacific Northwest of North America, China (Lushan), central Europe, Taiwan, and New Zealand [14,18–22].

Due to long-term weathering and erosion, older geological regions may have a high thickness of residual soil formation and colluvium soil deposits with fine soil particles. In addition, there are considerable differences in topography. Because of its young geology, the site-specific topography of Ikawa has a high-relief and high-valley density compared with that of Sabaragamuwa.

High-grade metamorphic rocks in the Sabaragamuwa area contain fine particles and exhibit systematic jointing with low intensity, resulting in the presence of large boulders mixed with clay soil. Additionally, the gentle slopes and wider valleys in the area facilitate the accumulation of large colluvium deposits and residual soil with considerable thickness, formed through historical landslide activity and long-term weathering [47,48]. In Ikawa, sedimentary rocks are highly fractured and jointed, with intense jointing. When typhoon precipitation hits the slopes, landslides occur, resulting in the collapse of slopes which contain small to medium-scale rock segments. The steep mountains associated with young geological ages do not favor the formation of thick soil deposits [49]. The characteristics of these materials and the thickness of the deposit may affect landslide phenomena.

Furthermore, the occurrence of landslides may have been influenced not only by site conditions but also by triggering factors such as rainfall patterns [50]. Table 1 shows that this study does not focus on landslides caused by a single event. The data covers landslides that occurred due to various events over a 10-year period which may include data on landslides that occurred due to various rainfall events, and there is a possibility the effects of rainfall have been removed. However, further investigation is required to determine the influence of climatic differences between regions on landslide phenomena.

Despite a notable difference in geological age, topography, materials, and climates between Ikawa and Sabaragamuwa, the scale of the landslide initiation area and initiation area slope angle were almost the same even though the flow and deposition part was different because of a significant difference in topography, as argued in the previous section.

5.4. Strengths, Limitations, and Future Prospects

This study illustrates different landslide geometrical characteristics in two geological settings and the topographical influence on landslide geometry. On the basis of these differences, we can argue that landslide risk analysis methods and simulations require site-specific adaptation before application. Nevertheless, note that this study is limited to two study areas. Therefore, these findings are not sufficiently conclusive to determine the primary factors that control landslide geometry and mobility in any other geological setting. However, this study provides evidence that landslides in these study areas exhibit different characteristics and mobility, with a clear association with the underlying geological formations and topography.

Various studies have emphasized the significance of incorporating landslide probability and mobility into hazard assessment and risk management strategies [37–39]. Landslide density is indicative of both the likelihood of landslide occurrence and the spatial distribution of landslide hazards. The size and mobility of landslides are crucial factors in determining the extent of the hazard area, making them important considerations in landslide hazard zonation mapping and mitigation strategies [51–54]. Numerous studies have been conducted to develop methods for assessing landslide occurrences. These methods include physically based models [55] and empirical models [56]. While these models provide valuable information about the spatial patterns of landslide susceptibility, there is still a lack of methods for predicting landslide size and mobility. Although the method used in this study is very simple, it is effective in characterizing landslide density, scale, and mobility. Moreover, it can be applied to many regions lacking field survey data and inventories of landslides. The comparative analysis not only enhances our understanding of landslide characteristics but also calls for broader research across diverse regions for comprehensive insights into landslide patterns and risk mitigation strategies.

Recently, numerous researchers have highlighted the impact of climate change on landslide activities [41,57]. However, as Gariano and Guzzetti (2016) [58] pointed out, there are limited studies that provide data on the effects of climate change on landslides, except for a few countries. This study presents a simple method for compiling landslide inventories using archived satellite images from the last decade. We believe that these efforts will provide us with new information on the relationship between climate change and landslide activity in different regions.

6. Conclusions

Landslides, a natural disaster causing fatalities, infrastructure damage, and economic losses globally in mountainous regions, prompt the need for mitigation measures in these vulnerable areas. However, the absence of landslide inventory data for certain regions typically leads to a reliance on risk analysis methods and simulations developed elsewhere. Challenges in data acquisition due to access difficulties and high costs contribute to the lack of landslide information.

This study offered valuable insights into the applicability of Google Earth satellite images as a cost-effective remote-sensing method for collecting landslide geometrical data. The reasonable resolution of current Google Earth images facilitated the identification of landslide features. Benefiting from these advantages, this study highlighted that Ikawa Mountain in Japan exhibited higher landslide density and a tendency for multiple landslides than Sabaragamuwa. Furthermore, a comparison of landslide characteristics between Ikawa and Sabaragamuwa indicated similar initiation areas; however, Sabaragamuwa experienced more widespread and mobile landslides. These variations can be attributed to topography. The landslide spread area and travel distance are crucial for determining the vulnerable areas in these selected regions. Therefore, this study underscored the importance of site-specific adaptation in landslide risk analysis methods and simulations for effective risk management.

This study was limited to two geological settings and their related topography and climate conditions. Therefore, there is a need to extend the comparison of landslide characteristics to multiple geological settings for a more comprehensive understanding of the controlling factors influencing landslide geometry and characteristics.

Author Contributions: Conceptualization, S.N, T.U and Y.Y.; methodology, S.N, T.U and Y.Y.; software, S.N., A.K. and M.H.; validation, S.N. and T.U.; formal analysis, S.N.; investigation, S.N. and Y.Y.; resources, S.N. and Y.Y.; data curation, S.N.; writing—original draft preparation, S.N.; writing—review and editing, S.N. and T.U.; visualization, S.N. and M.H.; supervision, T.U. and Y.Y.; project administration, T.U.; funding acquisition, S.N. and T.U. All authors have read and agreed to the published version of the manuscript.

Funding: This research was funded in part by the Project for Human Resources Development Scholarship by the Japanese Grant Aid (JDS), Japan International Cooperation Agency (JICA) and JSPS KAKENHI Grant JP20H03019.

Data Availability Statement: The raw data supporting the conclusions of this article will be made available by the authors on request.

Acknowledgments: The authors would like to express appreciation for the valuable comments of the associated editors and anonymous reviewers.

Conflicts of Interest: The authors declare no conflict of interest.

References

1. Hervás, J. *Lessons Learnt from Landslide Disasters in Europe*; European Communities: Luxembourg, 2003; p. 91.
2. Dai, F.C.; Chin, F.L.; Ngai, Y.Y. Landslide risk assessment and management: An overview. *Eng. Geol.* **2002**, *64*, 65–87. [CrossRef]
3. Matthias, J.; Steven, L. Climate change effects on landslides along the southwest coast of British Columbia. *Geomorphology* **2009**, *107*, 275–284. [CrossRef]
4. Cruden, D.M.; Varnes, D.J. Landslide Types and Processes, Transportation Research Board, U.S. National Academy of Sciences. *Spec. Rep.* **1996**, *247*, 36–75.
5. Bessette-Kirton, E.K.; Coe, J.A.; Schulz, W.H.; Cerovski-Darriau, C.; Einbund, M.M. Mobility characteristics of debris slides and flows triggered by Hurricane Maria in Puerto Rico. *Landslides* **2020**, *17*, 2795–2809. [CrossRef]
6. Onda, Y. *Underlying Rock Type Controls of Hydrological Processes and Shallow Landslide Occurrence*; IAHS Publication: Wallingford, UK, 1993; p. 47.
7. Chen, X.; Wang, M.; Chuan, Y.; Wei, Y.; Zhang, P.; Chen, M.T. Topographic controls on the distribution of coseismic landslides: A case study using the coefficient of variation of the 2014 Ludian, Yunnan, China, Ms6.5 Earthquake. *Lithosphere* **2022**, *2021*, 6678652. [CrossRef]
8. Borgomeo, E.; Hebditch, K.V.; Whittaker, A.C.; Lonergan, L. Characterising the spatial distribution, frequency and geomorphic controls on landslide occurrence, Molise, Italy. *Geomorphology* **2014**, *226*, 148–161. [CrossRef]
9. Avanzi, G.D.A.; Giannecchini, R.; Puccinelli, A. The influence of the geological and geomorphological settings on shallow landslides. An example in a temperate climate environment: The June 19, 1996 event in northwestern Tuscany (Italy). *Eng. Geol.* **2004**, *73*, 215–228. [CrossRef]
10. Alkhasawneh, M.; Ngah, U.K.; Tay, L.T.; Mat Isa, N.A.; Al-batah, M.S. Determination of important topographic factors for landslide mapping analysis using MLP network. *Sci. World J.* **2013**, *2013*, 415023. [CrossRef] [PubMed] [PubMed Central]
11. Nakileza, B.R.; Nedala, S. Topographic influence on landslides characteristics and implication for risk management in upper Manafwa catchment, Mt Elgon Uganda. *Geoenviron. Disasters* **2020**, *7*, 27. [CrossRef]

12. Gao, J.; Maro, J. Topographic controls on evolution of shallow landslides in pastoral Wairarapa, New Zealand, 1979–2003. *Geomorphology* **2010**, *114*, 373–381. [CrossRef]
13. Zhang, F.; Chen, W.; Liu, G.; Liang, S.; Kang, C.; He, F. Relationships between landslide types and topographic attributes in a loess catchment, China. *J. Mt. Sci.* **2012**, *9*, 742–751. [CrossRef]
14. Rana, K.; Ugur, O.; Nishant, M. Landslide geometry reveals its trigger. *Geophys. Res. Lett.* **2021**, *48*, e2020GL090848. [CrossRef]
15. Frattini, P.; Crosta, G.B. The role of material properties and landscape morphology on landslide size distributions. *Earth Planet. Sci. Lett.* **2013**, *361*, 310–319. [CrossRef]
16. Schneider, D.; Huggel, C.; Haeberli, W.; Kaitna, R. Unraveling driving factors for large rock–ice avalanche mobility. *Earth Surf. Process. Landf.* **2011**, *36*, 1948–1966. [CrossRef]
17. Kasai, M.; Yamada, T. Topographic effects on frequency-size distribution of landslides triggered by the Hokkaido Eastern Iburi Earthquake in 2018. *Earth Planets Space* **2019**, *71*, 89. [CrossRef]
18. Taylor, F.E.; Malamud, B.D.; Witt, A.; Guzzetti, F. Landslide shape, ellipticity and length-to-width ratios. *Earth Surf. Process. Landf.* **2018**, *43*, 3164–3189. [CrossRef]
19. Xu, C.; Xiwei, X.; Bruce, J.; Shyu, H. Database and spatial distribution of landslides triggered by the Lushan, China Mw 6.6 earthquake of 20 April 2013. *Geomorphology* **2015**, *248*, 77–92. [CrossRef]
20. Bernat Gazibara, S.; Krkač, M.; Mihalić Arbanas, S. Landslide inventory mapping using LiDAR data in the City of Zagreb (Croatia). *J. Maps* **2019**, *15*, 773–779. [CrossRef]
21. Wu, C. Using the spatiotemporal hot spot analysis and multi-annual landslide inventories to analyze the evolution and characteristic of rainfall-induced landslide at the subwatershed scale in Taiwan. *Water* **2023**, *15*, 1355. [CrossRef]
22. Korup, O. Distribution of landslides in southwest New Zealand. *Landslides* **2005**, *2*, 43–51. [CrossRef]
23. Nichol, J.; Wong, M.S. Satellite remote sensing for detailed landslide inventories using change detection and image fusion. *Int. J. Remote Sens.* **2005**, *26*, 1913–1926. [CrossRef]
24. Đurić, D.; Mladenović, A.; Pešić-Georgiadis, M.; Marjanović, M.; Abolmasov, B. Using multiresolution and multitemporal satellite data for post-disaster landslide inventory in the Republic of Serbia. *Landslides* **2017**, *14*, 1467–1482. [CrossRef]
25. Lissak, C.; Bartsch, A.; De Michele, M.; Gomez, C.; Maquaire, O.; Raucoules, D.; Roulland, T. Remote sensing for assessing landslides and associated hazards. *Surv. Geophys.* **2020**, *41*, 1391–1435. [CrossRef]
26. Casagli, N.; Intrieri, E.; Tofani, V.; Gigli, G.; Raspini, F. Landslide detection, monitoring and prediction with remote-sensing techniques. *Nat. Rev. Earth Environ.* **2023**, *4*, 51–64. [CrossRef]
27. Mohan, A.; Singh, A.K.; Kumar, B.; Dwivedi, R. Review on remote sensing methods for landslide detection using machine and deep learning. *Trans. Emerg. Telecommun. Technol.* **2021**, *32*, 3998. [CrossRef]
28. Sato, H.P.; Harp, E.L. Interpretation of earthquake-induced landslides triggered by the 12 May 2008, M7. 9 Wenchuan earthquake in the Beichuan area, Sichuan Province, China using satellite imagery and Google Earth. *Landslides* **2009**, *6*, 153–159. [CrossRef]
29. Sato, H.P.; Hasegawa, H.; Fujiwara, S.; Tobita, M.; Koarai, M.; Une, H.; Iwahashi, J. Interpretation of landslide distribution triggered by the 2005 Northern Pakistan earthquake using SPOT 5 imagery. *Landslides* **2007**, *4*, 113–122. [CrossRef]
30. Mohammed, N.Z.; Ghazi, A.; Mustafa, H.E. Positional accuracy testing of Google Earth. *Int. J. Multidiscip. Sci. Eng.* **2013**, *4*, 6–9.
31. Farah, A.; Algarni, D. Positional accuracy assessment of GoogleEarth in Riyadh. *Artif. Satell.* **2014**, *49*, 101–106. [CrossRef]
32. Goudarzi, M.A.; Landry, R.J. Assessing horizontal positional accuracy of Google Earth imagery in the city of Montreal, Canada. *Geod. Cartogr.* **2017**, *43*, 56–65. [CrossRef]
33. Wirth, J.; Bonugli, E.; Freund, M. *Assessment of the Accuracy of Google Earth Imagery for Use as a Tool in Accident Reconstruction*; SAE Technical Paper, (No. 2015-01-1435); Biodynamic Research Corp.: San Antonio, TX, USA, 2015.
34. Handwerger, A.L.; Huang, M.H.; Jones, S.Y.; Amatya, P.; Kerner, H.R.; Kirschbaum, D.B. Generating landslide density heatmaps for rapid detection using open-access satellite radar data in Google Earth Engine. *Nat. Hazards Earth Syst. Sci.* **2022**, *22*, 753–773. [CrossRef]
35. Cooray, P.G. The Precambrian of Sri Lanka: A historical review. *Precambrian Res.* **1994**, *66*, 3–18. [CrossRef]
36. Kehelpannala, K.V.W. Deformation of a High-Grade Gondwana Fragment, Sri Lanka. *Int. Assoc. Gondwana Res. Jpn.* **1997**, *1*, 47–68. [CrossRef]
37. Konagai, K.; Karunawardena, A.; Bandara, K.N.; Sassa, K.; Onishi, R.; Uzuoka, R.; Asano, S.; Sasahara, K.; Jayakody, S.; Ariyarathna, I. Early warning system against rainfall-induced landslide in Sri Lanka. In *Progress in Landslide Research and Technology*; Springer International Publishing: Cham, Switzerland, 2023; Volume 1, pp. 217–235. [CrossRef]
38. Hemasinghe, H.; Rangali, R.S.; Deshapriya, N.L.; Samarakoon, L. Landslide susceptibility mapping using logistic regression model (a case study in Badulla District, Sri Lanka). *Procedia Eng.* **2018**, *212*, 1046–1053. [CrossRef]
39. Perera, E.N.C.; Gunaratne, A.M.C.T.; Samarasinghe, S.B.D. Participatory Landslide Inventory (PLI): An Online Tool for the Development of a Landslide Inventory. *Complexity* **2022**, *2022*, 2659203. [CrossRef]
40. Marambe, B.; Punyawardena, R.; Silva, P.; Premalal, S.; Rathnabharathie, V.; Kekulandala, B.; Nidumolu, U.; Howden, M. Climate, climate risk, and food security in Sri Lanka: The need for strengthening adaptation strategies. In *Handbook of Climate Change Adaptation*; Springer: Berlin/Heidelberg, Germany, 2015; pp. 1759–1789. [CrossRef]
41. Ratnayake, U.; Herath, S. Changing rainfall and its impact on landslides in Sri Lanka. *J. Mt. Sci.* **2005**, *2*, 218–224. [CrossRef]
42. Nisansala, W.D.S.; Abeysingha, N.S.; Islam, A.; Bandara, A.M.K.R. Recent rainfall trend over Sri Lanka (1987–2017). *Int. J. Climatol.* **2020**, *40*, 3417–3435. [CrossRef]

43. Murillo-García, F.G.; Alcántara-Ayala, I.; Ardizzone, F.; Cardinali, M.; Fiourucci, F.; Guzzetti, F. Satellite stereoscopic pair images of very high resolution: A step forward for the development of landslide inventories. *Landslides* **2015**, *12*, 277–291. [CrossRef]
44. Zhang, J.; Gurung, D.R.; Liu, R.; Murthy, M.S.R.; Su, F. Abe Barek landslide and landslide susceptibility assessment in Badakhshan Province, Afghanistan. *Landslides* **2015**, *12*, 597–609. [CrossRef]
45. Psomiadis, E.; Papazachariou, A.; Soulis, K.X.; Alexiou, D.S.; Charalampopoulos, I. Landslide mapping and susceptibility assessment using geospatial analysis and earth observation data. *Land* **2020**, *9*, 133. [CrossRef]
46. Henriques, C.; Zêzere, J.L.; Marques, F. The role of the lithological setting on the landslide pattern and distribution. *Eng. Geol.* **2015**, *189*, 17–31. [CrossRef]
47. Katupotha, J. *Geomorphic Surfaces of the River Basins in the Western and Southern Parts of Sri Lanka*; Natural Resources, Energy and Science Authority of Sri Lanka: Colombo, Sri Lanka, 2015. [CrossRef]
48. Osanai, Y.; Sajeev, K.; Owada, M.; Kehelpannala, K.W.; Prame, W.B.; Nakano, N.; Jayatileke, S. Metamorphic evolution of high-pressure and ultrahigh-temperature granulites from the Highland Complex, Sri Lanka. *J. Asian Earth Sci.* **2006**, *28*, 20–37. [CrossRef]
49. Saito, H.; Nakayama, D.; Matsuyama, H. Comparison of landslide susceptibility based on a decision-tree model and actual landslide occurrence: The Akaishi Mountains, Japan. *Geomorphology* **2009**, *109*, 108–121. [CrossRef]
50. Tatard, L.; Grasso, J.R.; Helmstetter, A.; Garambois, S. Characterization and comparison of landslide triggering in different tectonic and climatic settings. *J. Geophys. Res. Earth Surf.* **2010**, *115*, F04040. [CrossRef]
51. Legros, F. The mobility of long-runout landslides. *Eng. Geol.* **2002**, *63*, 301–331. [CrossRef]
52. Iverson, R.M.; George, D.L.; Allstadt, K.; Reid, M.E.; Collins, B.D.; Vallance, J.W.; Schilling, S.P.; Godt, J.W.; Cannon, C.M.; Magirl, C.S.; et al. Landslide mobility and hazards: Implications of the 2014 Oso disaster. *Earth Planet. Sci. Lett.* **2015**, *412*, 197–208. [CrossRef]
53. Düzgün, H.S.B.; Özdemir, A. Landslide risk assessment and management by decision analytical procedure for Dereköy, Konya, Turkey. *Nat. Hazards* **2006**, *39*, 245–263. [CrossRef]
54. Amarasinghe, M.P.; Kulathilaka, S.A.S.; Robert, D.J.; Zhou, A.; Jayathissa, H.A.G. Risk assessment and management of rainfall-induced landslides in tropical regions: A review. *Nat. Hazards* **2023**, *120*, 2179–2231. [CrossRef]
55. Jiang, Y.; Hu, X.; Liang, H.; Ning, P.; Fan, X. A Physically Based Model for the Sequential Evolution Analysis of Rainfall-Induced Shallow Landslides in a Catchment. *Water Resour. Res.* **2023**, *59*, e2022WR032716. [CrossRef]
56. Bera, A.; Mukhopadhyay, B.P.; Das, D. Landslide hazard zonation mapping using multi-criteria analysis with the help of GIS techniques: A case study from Eastern Himalayas, Namchi, South Sikkim. *Nat. Hazards* **2019**, *96*, 935–959. [CrossRef]
57. Uchida, T.; Sakurai, W.; Okamoto, A. Historical Patterns of Heavy Rainfall Event and Deep-Seated Rapid Landslide Occurrence in Japan: Insight for Effects of Cli-mate Change on Landslide Occurrence. In *Advancing Culture of Living with Landslides: Diversity of Landslide Forms*; Springer International Publishing: Berlin/Heidelberg, Germany, 2017; Volume 4, pp. 251–257. [CrossRef]
58. Gariano, S.L.; Guzzetti, F. Landslides in a changing climate. *Earth-Sci. Rev.* **2016**, *162*, 227–252. [CrossRef]